Assessment of the Role of an Ω Loop of Cholesterol Oxidase: A Truncated Loop Mutant Has Altered Substrate Specificity†

Nicole S. Sampson,* Ignatius J. Kass, and Kajal Bose Ghoshroy‡

Department of Chemistry, State University of New York, Stony Brook, New York 11794-3400

Received December 12, 1997; Revised Manuscript Received February 23, 1998

ABSTRACT: The function of an active site loop (70−90) of cholesterol oxidase has been ascertained by deleting five contiguous residues (79−83) from the tip of the loop. From the crystal structure of the wild-type enzyme, it appears that this truncation will not significantly perturb the structure of the rest of the enzyme. The UV/vis and CD spectra of the mutant confirm that the enzyme is properly folded with FAD bound. The mutant enzyme still transfers ^{2}H from the 4β-carbon of the intermediate, cholest-5-en-3-one, to the 6β-carbon of the product, cholest-4-en-3-one, during isomerization. The k_{cat}/K_m of the mutant is increased 6-fold with dehydroepiandrosterone as substrate. Thus, the enzyme is still catalytically active after deletion of the five loop-tip residues. With micellar cholesterol, the k_{cat}/K_m of the mutant is decreased 170-fold relative to wild type. This suggests that the tip of the loop is necessary for packing with the "tail" of cholesterol and is responsible for substrate specificity at C_{17}. Increased release of intermediate cholest-5-en-3-one in the mutant-catalyzed reaction is not observed. Truncation of the loop, therefore, does not affect the grip of the enzyme on the intermediate. With lipid vesicle substrates (egg phosphatidylcholine/cholesterol, 1:1), the initial velocity of the mutant is reduced 3000-fold. The binding affinity for the vesicles, however, is only reduced 2-fold. Consequently, the loop is not the primary determinant of binding affinity for vesicles. It is concluded that the loop is important for movement of cholesterol from the lipid bilayer. The tip residues form a hydrophobic pathway between lipid membrane and active site to facilitate movement of substrate and product in to and out of the active site.

Many enzymes have an intrinsic flexibility essential for their function (*1*). Their degree of flexibility depends on the function of the enzyme and ranges from large domain movements to displacements of smaller segments. Comprised of contiguous segments of polypeptide, Ω loops, classified as nonregular secondary structure (*2*, *3*), often participate in catalysis as flexible elements.

Ω loops may exist in a variety of conformations and they have small end-to-end distances. They typically occur on the surfaces of proteins where they are well situated to participate in catalysis. Loop movement can occur on quite a large scale, and displacements of 10 Å are not unusual. First introduced by Koshland (*4*), the concept of "induced-fit" proposed that enzymes were flexible in order to recruit catalytic groups and to refine substrate recognition. [Note the caveats of this proposal discussed by Herschlag (*5*).] The importance of loop motion, a subset of induced-fit movement, has been tested experimentally in several systems. Holbrook and co-workers have elegantly demonstrated that closure of the active site loop of lactate dehydrogenase moves arginine 109 into hydrogen bonding distance of the substrate carbonyl (*6*). In addition, tyrosyl-tRNA synthetase and dihydrofolate reductase both have loops that help stabilize the transition state and destabilize the ground state (*7*, *8*).

X-ray structural analysis is the method by which the mobility of a loop is generally first revealed. If an enzyme loop crystallizes in different conformations with and without substrate analogues/inhibitors present, this is an indication that the loop has an important catalytic function. Assessment of the role that the loop actually plays then requires experimental confirmation. With deletion experiments, mobile loops have been shown to serve more diverse functions in catalysis than originally suggested. The flexible loop of glutathione synthetase aids in the recognition of glycine and prevents hydrolysis of the acyl phosphate reaction intermediate (*9*). The active site loop of triose-phosphate isomerase sequesters the reactive enediol(ate) intermediate in the active site. Furthermore, the loop constrains the intermediate in a planar cisoid conformation, to minimize phosphate elimination (*10*). Similarly, the active site loop of ribulose-1,5-bisphosphate carboxylase/oxygenase protects its enediol(ate) intermediate and also recruits an electropositive group to the active site (*11*). Loops also modulate activities of neighboring subunits and stabilize proteins and subunit interactions (*12*−*14*).

The majority of active site loops close in order to perform their function, e.g., sequester a reactive intermediate. There is a category of loop enzymes that function in the opposite manner, i.e., the open-loop form is the ligand-bound form. These enzymes have lipophilic substrates and, consequently,

† This work is supported by NIH Grant HL-53306 and in part by an American Heart Grant-in-Aid, a Camille and Henry Dreyfus New Faculty Award, and NSF MCB-9405394 (N.S.). I.J.K. is a DOE/GAANN fellow. K.B.G. is an American Heart Association−NY Affiliate postdoctoral fellow. The NMR spectroscopy facility at SUNY Stony Brook is supported by a grant from the NSF (CHE 9413510).

* To whom correspondence should be addressed. Telephone: (516) 632-7952. Fax: (516) 632-5731. E-mail: nicole.sampson@sunysb.edu.

‡ Present address: Department of Biology, Mississippi University for Women, P.O. Box W-100, Columbus, MS 39701.

S0006-2960(97)03067-5 CCC: $15.00
Published on Web 04/03/1998

Scheme 1: Reaction Catalyzed by Cholesterol Oxidase

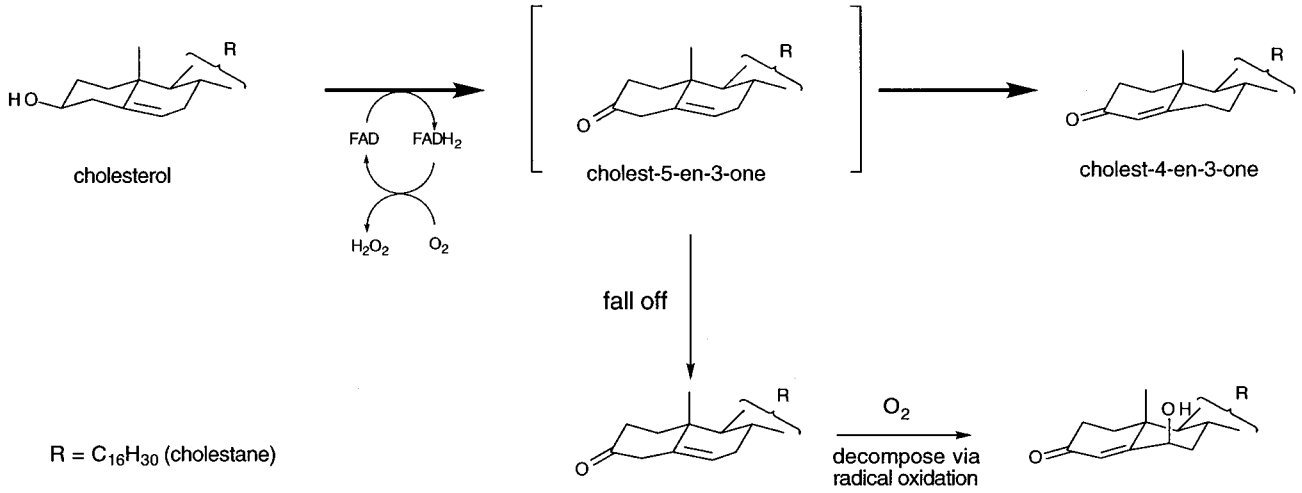

hydrophobic active sites. To prevent aggregation of these proteins, amphipathic loops cover their active sites. For example, both pancreatic and fungal lipases have active site lids, composed of α-helix and loop, that open to create a hydrophobic surface (*15*−*17*). This protein surface interacts with the surface of the lipid phase that contains the substrate. Without a lipid surface present to stabilize the open conformation, the lipases are very slow to process aggregated substrates.

In the present paper, we examine the role of a surface loop in the reaction catalyzed by cholesterol oxidase. Cholesterol oxidase (EC 1.1.3.6) catalyzes the oxidation and isomerization of cholesterol to form cholest-4-en-3-one (Scheme 1). The X-ray crystal structures of *Brevibacterium* cholesterol oxidase (choB) solved by Blow and co-workers (*18*, *19*) raise interesting questions about access to the active site by the substrate. The structures of the native enzyme and of the DHEA[1]-bound enzyme are very similar. In both structures, the active site is solvent inaccessible. Furthermore, the topology of the enzyme and the atomic temperature factors for residues in two surface loops suggest that the enzyme must undergo a conformational change involving 10−20 amino acid residues of these loops in order to bind substrate.

These surface loops (70−90, 433−437[2]) appear to cap the active site (Figure 1a). Although the conformation of the "open" enzyme is not known, we postulate that one or both of these loops open to form a hydrophobic pathway between the membrane and the active site. This pathway would lower the activation barrier for cholesterol movement out of the bilayer. Upon binding, the four rings of the sterol are completely buried in the substrate binding site. Because DHEA has a ketone at C_{17} (Chart 1), the loops can close over the substrate analogue and bury it. Presumably, when cholesterol is bound, the eight-carbon "tail" sticks out of the binding site and packs with the open loops. Part of the C_{17}-tail may be left in the membrane.

In this work, we undertook an assessment of the functional importance of the larger active site loop (70−90) (Chart 2) in catalysis and binding. To test the role of the loop, we constructed a deletion mutant of cholesterol oxidase. This mutant is missing five contiguous residues (79−83) from the tip of the loop (Figure 1b). The characterization of this deletion mutant and the catalytic consequences that occur as a result of loop truncation are presented below.

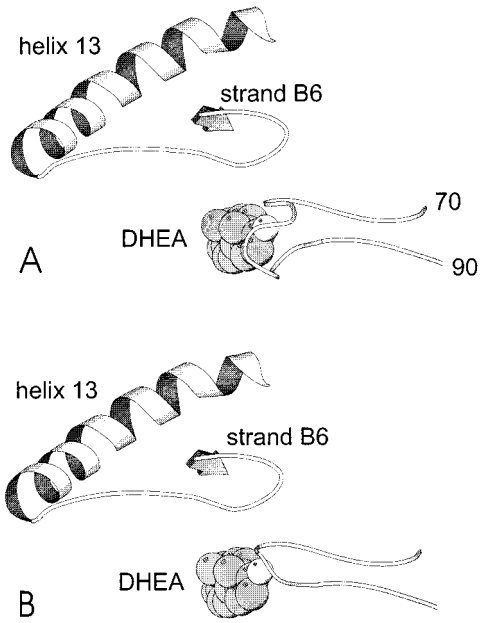

FIGURE 1: Drawings of cholesterol oxidase substrate binding site. Carbon is colored gray; heteroatoms are shown in white. In both drawings, the ketone at C_{17} is facing the viewer, and the 3-hydroxyl is behind the plane of the page. The drawings were generated by using MOLSCRIPT (*50*). (A) X-ray crystal structure of *B. sterolicum* cholesterol oxidase with DHEA bound in the active site (*18*, *19*). Coordinates were obtained from the Brookhaven Protein Data Bank (1COY). Loop 433−437 is between helix 13 and strand B6. (B) Model of Δ^{79-83} cholesterol oxidase created using InsightII (Biosym, Palo Alto, CA) shown in the same orientation as the wild-type structure.[2]

[1] Abbreviations: choB, *Brevibacterium sterolicum* cholesterol oxidase; choA, *Streptomyces* cholesterol oxidase; DHEA, dehydroepiandrosterone (3β-hydroxyandrost-5-en-17-one); ePC, egg phosphatidylcholine; LB, Luria broth; IPTG, isopropyl β-D-thiogalactoside; Tris, tris(hydroxymethyl)aminomethane; SDS−PAGE, sodium dodecyl sulfate polyacrylamide gel electrophoresis; DEAE, diethylaminoethyl; TEA, triethanolamine; EDTA, ethylenediaminetetraacetate; HPLC, high-pressure liquid chromatography.

[2] This numbering refers to the X-ray crystal structure system for numbering amino acid residues (*19*). Numbering begins at the N-terminus of the processed *Brevibacterium* enzyme. Residues 79−83 are encoded by codons 115−119 in the *Streptomyces* gene (*20*) and codons 124−128 in the *Brevibacterium* gene (*21*).

Chart 1: Structures of Cholesterol and DHEA

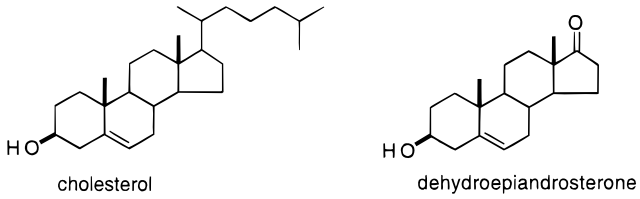

Chart 2: Schematic of the Active Site Loop of Cholesterol Oxidase[a]

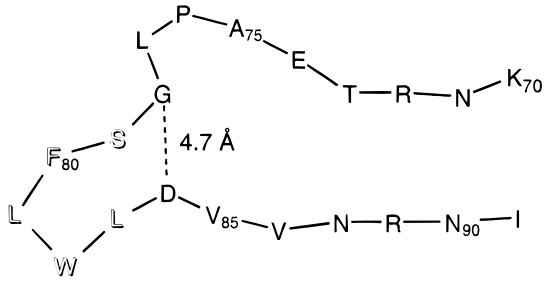

[a] The active site residues are highlighted.

EXPERIMENTAL PROCEDURES

Materials. Cholest-4-en-3-one and cholesterol were purchased from Sigma Chemical Co. (St. Louis, MO). ePC was purchased from Avanti Polar Lipids (Alabaster, AL). The plasmid for heterologous expression of *Streptomyces* cholesterol oxidase, pCO117, was a generous gift from Y. Murooka (*22*). Restriction endonucleases, T4 DNA ligase, Klenow fragment of DNA polymerase I, and T4 kinase were purchased from New England Biolabs (Beverly, MA). Oligonucleotides were purchased from IDT, Inc. (Coralville, IA). Unless otherwise specified, all chemicals and solvents, of reagent or HPLC grade, were supplied by Fisher Scientific (Pittsburgh, PA). Water for assays and chromatography was distilled, followed by passage through a Barnstead NANOpure filtration system to give a resistivity better than 18 MΩ.

General Methods. Vesicles were prepared with an extruder from Lipex Biomembranes Inc. (Vancouver, BC, Canada). A Shimadzu UV2101 PC Spectrophotometer was used for assays. Fluorescence measurements were taken on an I.S.S. K2 spectrofluorometer (Champaign, IL). Restriction digests and ligations were performed according to procedures described in Sambrook et al. (*23*) The buffers used were (A) 50 mM sodium phosphate, pH 7.0, (B) 50 mM sodium phosphate, pH 7.0, 0.025% Triton X-100, and (C) 45 mM sodium phosphate, pH 7.0, 10% EtOH.

Construction of pCO202 Expression Plasmid. The *Bam*HI to *Nde*I fragment of pCO117 (*22*) containing the *Streptomyces* cholesterol oxidase choA gene was subcloned into pUC19. Then the extraneous *Streptomyces* DNA between the OPA and the *Hind*III site was removed by PCR using two primers. Primer 1 was a 65-base oligonucelotide that included the *Mlu*I site within the choA gene and corresponded to the sequence of the coding strand (5′-CgCAgACgCgTgggACAACAgCgACTCCTCggTCTTCgCggAgATCgCCCCCATgCCggCCggCC-3′). Primer 2 was a 27-base oligonucleotide that encoded the last six codons of the choA gene, incorporated a *Hind*III site with the OPA codon, and was complementary to the coding strand (5′-gCAgCAAgCTTACgACgCCgTgACgTC-3′). Using *Xho*I restricted pCO117 as a template, 10 cycles of PCR were performed with Taq polymerase and an annealing temperature of 55 °C. The 500 bp PCR fragment was digested with *Mlu*I and *Hind*III, purified, and subcloned into pCO117 that had been similarly digested to yield the pCO202 expression plasmid containing the *Streptomyces* choA gene behind a tac promoter. The sequence of the 483 bp region of pCO202 synthesized by PCR was verified by ABI Prism dye terminator cycle sequencing, using the manufacturer's protocol (Perkin-Elmer, Foster City, CA).

Construction of Δ^{79-83} *Mutant Expression Plasmid, pCO222*. An 83-bp DNA fragment was synthesized that encoded the deletion mutation. This fragment was synthesized by using the Klenow fragment of DNA polymerase I and two primers. Primer 1 was an 83-base oligonucleotide that spanned the *Sph*I and *TthIII*1 sites, was missing the codons for amino acids 79−83,[2] and was complementary to the coding strand (5′-CCggTTgACgACgTCgCCgAgCggggCCTCggTgCggTTCTTgAACCAgCTggACCgCTTgTCCgggTTgAgCATgCCgCAgC-3′). Primer 2 was a 20-base oligonucleotide that included the *Sph*I restriction site and was complementary to primer 1 (5′-gCTgCggCATgCTCAACCCg-3′). The primers (100 μM each) were mixed in buffer (10 mM Tris-HCl, 5 mM $MgCl_2$, 7.5 mM DTT, pH 7.5 at 25 °C). The mixture was heated at 37 °C for 1 h and allowed to cool to room temperature over 1 h. Klenow fragment of DNA polymerase I (5 units) and deoxynucelotide triphosphates (100 μM each) were added and the reaction mixture was incubated at 37 °C for 3.5 h. The cassette was purified by phenol extraction and EtOH precipitation. The cassette was digested with *Sph*I and *TthIII*1 and purified by PAGE. The *Streptomyces* cholesterol oxidase gene in pCO202 was restricted with *Sph*I and *TthIII*1 and the fragments were purified by agarose gel electrophoresis. The cassette encoding the deletion was ligated into the 4483 bp fragment from the pCO202 digest to generate the expression plasmid containing mutant cholesterol oxidase, pCO222. The mutation was verified by dideoxy termination sequencing (*24*) of the cassette region of the pCO222 construct.

Purification of Wild-Type Cholesterol Oxidase. Cell paste of *E. coli* BL21(DE3)plysS(pCO117) obtained from LB-ampicillin (200 μg/mL) medium (grown at 30 °C for 12 h after addition of IPTG (0.2 mM) at $A_{600} = 0.7$ was purified as previously described (*25*). Protein concentrations were determined by UV absorbance using $\epsilon_{280} = 81\,924\ M^{-1}\ cm^{-1}$ (calculated from the molar extinction coefficients of tryptophan and tyrosine (*26*)).

Purification of Δ^{79-83} *Cholesterol Oxidase*. Cell paste of *E. coli* BL21(DE3)plysS(pCO222) obtained from LB-ampicillin (200 μg/mL) medium (1 L) grown for 10 h at 30 °C after addition of IPTG (0.2 mM) at $A_{600} = 0.7$ was resuspended in 50 mM Tris-HCl, 1 mM EDTA, pH 7 (30 mL), and lysed by French press at 16 000 psi. All subsequent purification steps were performed at 4 °C. Cell debris was removed by centrifugation at 135000*g* for 60 min. The supernatant was fractionated by the addition of $(NH_4)_2SO_4$. The pellet from a fractionation with 1.5 M $(NH_4)_2SO_4$ was discarded and $(NH_4)_2SO_4$ added to the supernatant to a final concentration of 2.5 M. This pellet was resuspended in buffer A (5 mL) and desalted by repeated dialysis against buffer A. The retentate was loaded onto a column of DEAE-cellulose (30 mm × 15 cm, DE-52, Whatman), preequili-

brated with buffer A, and eluted with the same buffer (80 mL, 10 mL fractions). Fractions containing cholesterol oxidase were concentrated by $(NH_4)_2SO_4$ precipitation (2.5 M), the pellet was redissolved in buffer A (1 mL), and $(NH_4)_2SO_4$ was slowly added to a final concentration of 2 M. The precipitate that formed was removed by centrifugation after 30 min, and the cholesterol oxidase allowed to crystallize over 2 days. The microcrystalline protein was collected by centrifugation and the pellet of cholesterol oxidase was dissolved in buffer A and ultrafiltered (YM30 membrane, Amicon, Inc., Danvers, MA) into buffer A. Purity was analyzed by SDS−PAGE. Typically, 3−5 mg of pure cholesterol oxidase were obtained per liter of culture. Protein concentrations were determined by UV absorbance using $\epsilon_{280} = 76\,365\ M^{-1}\ cm^{-1}$ (calculated from the molar extinction coefficients of tryptophan and tyrosine (*26*)).

UV and CD Spectra of Cholesterol Oxidase. A solution of cholesterol oxidase was prepared in buffer A. A baseline spectrum of buffer A was subtracted from the sample spectrum. The concentration of cholesterol oxidase was 15−19 μM for UV spectra and CD spectra in the near-UV. For CD spectra in the far-UV, the protein concentration was 58 μM (wild type) or 15 μM (mutant).

Synthesis of Lipid Vesicles. Medium, 100-nm unilamellar vesicles were made from mixtures of steroids and lipids by extrusion (*27*). Lipid (10 μmol) was mixed with steroid as a $CHCl_3$ solution in a round-bottomed flask, dried as a thin film under reduced pressure in a rotary evaporator for 20 min, and evacuated under high vacuum for 2 h. The lipid was resuspended in 1 mL of buffer A with vortexing. Five freeze−thaw cycles, at −80 and 37 °C, followed by 10 extrusion cycles through two stacked 100-nm filters (Costar) using a nitrogen gas pressure of 350−400 psi, provided a homogeneous batch of vesicles. Phospholipid concentrations of vesicle solutions were measured by using the Stewart assay (*28*). Cholesterol concentrations were measured by lysing vesicles with 0.1% Triton X-100 and using cholesterol oxidase to quantitate total cholesterol concentration as described below.

Activity Assay of Cholesterol Oxidase. The activity of wild-type cholesterol oxidase was measured by following the appearance of conjugated enone at 240 nm ($\epsilon_{240} = 12\,100\ M^{-1}\ cm^{-1}$ (*29*)). The activity also was determined by using a horseradish peroxidase coupled assay to quantitate the rate of formation of H_2O_2. The formation of quinoneimine at 510 nm was followed as a function of time. The standard assay conditions were the same as the UV A_{240} assay with the addition of 1.13 mM phenol, 0.87 mM 4-aminoantipyrine (Aldrich, Milwaukee, WI), and 10 units of horseradish peroxidase (Sigma, St. Louis, MO). When cholesterol was used as a substrate, it was added as a propan-2-ol solution to buffer B or as phospholipid vesicles to buffer A at 37 °C. DHEA was added as a solution in buffer C to buffer C at 37 °C. When alcohol solvents were used, the final assay mixtures were 2% propan-2-ol or 10% EtOH. Dilute enzyme stock solutions contained 200 μg/mL BSA. Assays with cholesterol in buffer A or DHEA in buffer C contained 200 μg/mL BSA.

Fluorescence Binding Measurements. Binding of cholesterol oxidase to vesicles was assayed through the quenching of intrinsic tryptophan fluorescence. All binding assays were conducted in buffer A, ambient temperature. Cuvettes were silanized to prevent adhesion of the protein to cuvette walls. Tryptophan was excited at 280 nm and spectra were collected from 310 to 450 nm. Cutoff filters (310 nm) were placed before the emission monochromator to reduce scattered light. Sample signals were corrected for light fluctuations by simultaneously monitoring the exciting light on a reference photomultiplier. Protein (5−10 μg/mL) was titrated with increasing amounts of lipid vesicles (0−100 μL of 3.3 mM) to a final concentration of 500 μM. Emission was corrected for any background signal by performing a titration in the absence of protein.

Binding constants were analyzed by first correcting spectra for dilution and background signal. The spectra were integrated and normalized to their value in the absence of added lipid. The adsorption isotherm was fitted to a hyperbolic function using KaleidaGraph software (Synergy Software, Reading, PA) and eq 1:

$$\Delta F = (F_{max}[L])/([L] + K_D) \quad (1)$$

where [L] is the lipid concentration, K_D the dissociation constant, ΔF the change in fluorescence intensity, and F_{max} the maximum change in fluorescence intensity.

HPLC Analysis. Samples were analyzed as previously described (*30*) with a model 680 gradient controller, three M510 solvent pumps, and a model 490 multiwavelength detector (Waters Corporation, Milford, MA) or a model PDA-1 photodiode array detector (Rainin Instrument, Woburn, MA). The following conditions were used: stationary phase, Microsorb-MV C-18 column (Rainin Instrument Corp., Woburn, MA, 5 μm, 10 Å, 4.6 × 250 mm); gradient elution at 1.25 mL/min; solvent A, CH_3CN; solvent B, propan-2-ol; solvent C, CH_3CN/H_2O (1:1, v/v); and detection at 212 and 240 nm. A 25-min isocratic elution with 80% A and 20% C, followed by a 10-min linear gradient to 85% A and 15% B, followed by a 25-min isocratic elution under the same conditions was used to separate the steroids. Samples were injected directly from assay solutions. The identity of the peaks was established by co-injection with authentic standards. Product ratios were determined by integration of peak areas as detected at 212 and 240 nm.

Determination of Reaction Stereospecificity. Deuterium labeling experiments were conducted as previously described (*31*). [4β-^{2}H]cholesterol (100 μM) was incubated with 21 μg of Δ^{79-83} cholesterol oxidase in 3 mL of buffer A. The [4β-^{2}H]cholesterol was 97 (± 2) % deuterium. The products were isolated by HPLC and analyzed by EI mass spectrometry. The position of deuterium incorporation in the product cholest-4-en-3-one was determined by integration of ^{1}H resonances and appearance of ^{2}H−^{13}C coupling in the ^{13}C NMR spectra.

RESULTS

Preparation of Δ^{79-83} Cholesterol Oxidase Mutant. The pCO202 plasmid was constructed in order to increase plasmid yields. The Δ^{79-83} point mutation was prepared by cassette mutagenesis using existing restriction sites in pCO202. The mutant cholesterol oxidase was heterologously expressed in *E. coli* at lower levels than wild-type cholesterol oxidase (5 mg/L vs 30 mg/L of culture). The mutant cholesterol oxidase was purified in a manner similar to wild type. Evidence that the mutant cholesterol oxidase is properly folded is

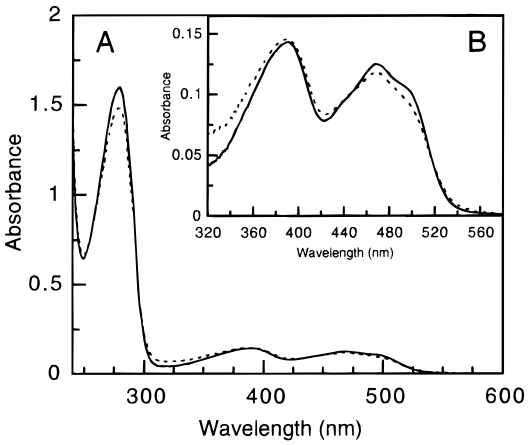

FIGURE 2: UV spectra of 19 μM wild-type (—) and 16 μM Δ^{79-83} (- - -) cholesterol oxidase in sodium phosphate buffer, pH 7.0. Spectra were normalized at 280 nm by using their calculated molar absorption coefficients. (A) Spectra from 240 to 600 nm. (B, inset) Close up of FAD region, from 320 to 580 nm.

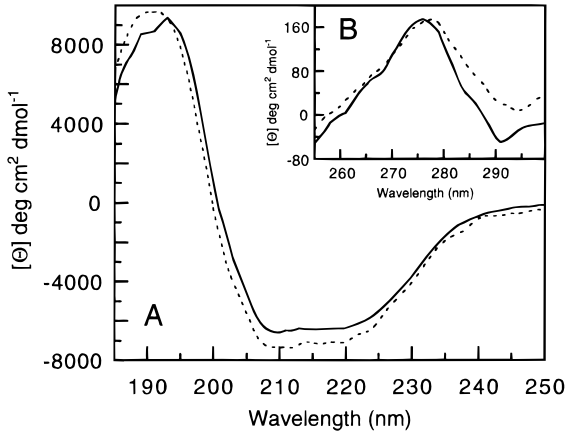

FIGURE 3: CD spectra of wild-type (—) and Δ^{79-83} (- - -) cholesterol oxidase in sodium phosphate buffer, pH 7.0. (A) Spectra from 180 to 250 nm of 58 μM wild-type and 16 μM Δ^{79-83} cholesterol oxidase. (B, inset) Spectra from 250 to 300 nm of 13 μM wild-type and 16 μM Δ^{79-83} cholesterol oxidase.

presented in Figures 2 and 3. The absorption at 280 nm of Δ^{79-83} is 7% lower than wild type; the FAD absorbance at 391 nm was used as an internal reference. This difference is expected because the Δ^{79-83} mutant has nine tryptophans, whereas wild type has 10. The UV spectra of the bound FAD cofactors have identical λ_{max}'s at 391 and 468 nm. The ratios of A_{280}/A_{391} and A_{280}/A_{468} are 11.1 and 12.8 for wild type and 10.1 and 12.5 for Δ^{79-83}, respectively. The CD spectra show that the enzyme is a mixture of α-helix and β-sheet, as expected from the X-ray crystal structure. The molar ellipticities are the same for wild type and Δ^{79-83} throughout the far- and near-UV.

Measurement of Catalytic Activity. The Michaelis−Menten parameters using both cholesterol and DHEA as substrates are reported in Table 1. The initial velocity at saturated binding to ePC/cholesterol (1:1) vesicles is reported in Table 2.

Analysis of Product Formed by Δ^{79-83}. Comparisons of Δ^{79-83} activity were made by measuring the rate of H_2O_2 formation by using the horseradish peroxidase coupled assay and by following the rate of cholest-4-en-3-one appearance at 240 nm. In the Δ^{79-83} catalyzed reaction, the two assays measure identical rates. This result implies that the product formed is cholest-4-en-3-one. The reaction product(s) was analyzed by reversed-phase C-18 HPLC using ^{14}C-labeled cholesterol. The major product observed was cholest-4-en-3-one (98%). The remaining 2% of the product was 6-hydroxycholest-4-en-3-one. This is the same product composition observed in the reaction catalyzed by wild-type cholesterol oxidase (*30*).

Binding of Cholesterol Oxidase to Lipid Bilayer. We measured the affinity of cholesterol oxidase for the lipid bilayer using quenching of the intrinsic tryptophan fluorescence of the protein as a reporter signal. After correction for vesicle light scattering and enzyme dilution, the data were fit to a hyperbolic isotherm. These results are summarized in Table 2.

We tested the activity of cholesterol oxidase with ePC/cholesterol 1:1 vesicles as substrate. Upon addition of increasing concentrations of ePC/cholesterol vesicles, the initial velocity increased and then saturated, indicating that cholesterol oxidase binds to vesicles. Relative initial velocities were plotted versus vesicle concentration and fit to eq 2 to obtain the apparent K_D for ePC/cholesterol (1:1).

$$v_i/v_{max} = [L]/\{[L] + K_D\} \quad (2)$$

[L] is the lipid concentration of ePC/cholesterol 1:1 vesicles, K_D the apparent dissociation constant for ePC/cholesterol 1:1 vesicles and cholesterol oxidase, v_i the initial velocity of product formation, and v_{max} the maximum initial velocity of product formation.

Measurement of ^2H Transfer. [4β-^{2}H]Cholesterol was incubated with recombinant *Streptomyces* wild-type cholesterol oxidase or Δ^{79-83} cholesterol oxidase and the product purified by reversed-phase HPLC for analysis. The percent deuterium remaining in the product cholest-4-en-3-one was determined by mass spectrometry. The product of the wild-type reaction contained 30% deuterium. ^{1}H NMR and ^{13}C NMR spectral analysis of the cholest-4-en-3-one revealed that the deuterium label transferred to the product was incorporated at the 6β-position of cholest-4-en-3-one. No deuterium label remained at carbon-4. The product of the mutant Δ^{79-83} reaction was the same as that of the wild-type reaction, except that it contained 22% deuterium at the 6β-position.

DISCUSSION

Cholesterol oxidase is part of a bacterial metabolic pathway for utilizing cholesterol as a carbon source. It is secreted by gram-positive bacteria, including *B. sterolicum* and *Streptomyces*. It was first isolated for use in serum cholesterol assays and subsequently was found to have larvicidal properties (*32*, *33*). It is also used as a probe of membrane structure (*34*).

Cholesterol oxidase catalyzes the conversion of cholesterol to cholest-4-en-3-one when cholesterol is presented in the lipid phase as part of a lipid bilayer or in the aggregated form as detergent micelles prepared with Triton X-100 and propan-2-ol. The lack of accessibility of the substrate binding site to the surface of the protein and bulk solution suggests that one or two loops must open during the substrate binding process (Figure 1a). We have used the *B. sterolicum* structure to guide our mutagenesis studies with the *Streptomyces* enzyme. The *B. sterolicum* and *Streptomyces*

Table 1: Michaelis−Menten Rate Constants for Wild-Type and Δ^{79-83} Cholesterol Oxidase

	cholesterol[a]			dehydroepiandrosterone[b]		
	k_{cat} (s^{-1})	K_m (μM)	$(k_{cat}/K_m)_{mut}/(k_{cat}/K_m)_{wt}$	k_{cat} (s^{-1})	K_m (μM)	$(k_{cat}/K_m)_{mut}/(k_{cat}/K_m)_{wt}$
wild type	76 ± 10	5 ± 1		0.69 ± 0.01	27.5 ± 0.5	
Δ^{79-83}	6 ± 2	70 ± 8	0.006	0.88 ± 0.02	6.3 ± 0.1	5.6

[a] Assays conducted in 50 mM sodium phosphate, pH 7.0, 0.025% Triton X-100, 2% propan-2-ol at 37 °C. [b] Assays conducted in 50 mM sodium phosphate, pH 7.0, 10% EtOH, 37 °C.

Table 2: Rate and Binding Constants for Wild-Type and Δ^{79-83} Cholesterol Oxidase with 100 nm Vesicles

	K_D for ePC (μM)[a]	apparent K_D for ePC/cholesterol (1:1) (μM)[b]	initial velocity for ePC/cholesterol (1:1) (s^{-1})[b]
wild type	87 ± 20	57 ± 21	24 ± 6
Δ^{79-83}	183 ± 39	147 ± 53	0.0087 ± 0.0002

[a] Determined by fluorescence. [b] Determined kinetically.

cholesterol oxidases are 58% and 64% identical in amino acid sequence and nucleotide sequence, respectively (*21*). The residues of the large loop (70−90) are 25% identical and 70% similar. Most importantly, in both enzymes, the outside face of the loop is hydrophilic and the inside face consists of hydrophobic amino acids. Thus the loop is amphipathic. In this work, we focused on the looplet formed by residues 79−83. The α-carbons of glycine 78 and aspartate 84 are approximately 4.7 Å apart (Chart 2). Thus, forming an amide bond between them should not severely perturb the overall structure of the protein. We genetically deleted residues 79−83 to create a mutant with an amide linkage between glycine 78 and aspartate 84 (Figure 1b). The glycine at position 78 allows minor structural adjustments to accommodate the deletion without incurring enthalpic penalties for unfavorable side-chain conformations.

We constructed the Δ^{79-83} deletion mutant by cassette mutagenesis, using two existing restriction sites, 77 bp apart. The Δ^{79-83} mutant was expressed at lower levels in *E. coli* than wild type (5 vs 30 mg/L). The enzyme that was produced, however, was properly folded with FAD bound. The UV/vis spectrum of the mutant has the same λ_{max} values for the FAD ring as wild type. The absorbance at 280 nm is 7% lower as expected upon deletion of tryptophan 82. The CD spectrum in the far- and near-UV is very similar to that of wild type (Figure 3). The protein is a mixture of α-helix and β-sheet.

We analyzed the product composition of the Δ^{79-83} catalyzed reaction in two ways. First, the reaction rate was measured with two different assays. One assay measures the appearance of cholest-4-en-3-one by following the increase in absorbance at 240 nm. This assay serves as a measure of the rate of oxidation and isomerization. The other assay measures the appearance of H_2O_2 by coupling the reaction with horseradish peroxidase. This assay determines the rate of FAD turnover and thus the rate of oxidation alone. We knew, from previous experiments, that the intermediate cholest-5-en-3-one, formed by oxidation of cholesterol, is released from the enzyme if the isomerization reaction is blocked (*30*). The off-rate for cholest-5-en-3-one is at most 20-fold slower than the off-rate for cholest-4-en-3-one. For enzymes whose loops are responsible for sequestering intermediate, e.g., triosephosphate isomerase or ribulose-1,5-bisphosphate carboxylase/oxygenase, deletion of part of the active-site loop increases the amount of reaction intermediate lost from the active site during turnover (*10*, *11*). Comparison of the reaction rates measured in the two cholesterol oxidase assays demonstrated that the rate of H_2O_2 production equals the rate of cholest-4-en-3-one production. This experiment suggested that cholest-4-en-3-one is the product of the Δ^{79-83} catalyzed reaction and that cholest-5-en-3-one was not the major product formed; i.e., the intermediate is *not* released from the enzyme as a consequence of loop truncation. The product composition was also analyzed directly by HPLC. This analysis clearly showed that 98% of the product was cholest-4-en-3-one and 2% was 6-hydroxycholest-4-en-3-one. An identical mixture is obtained upon reaction of cholesterol with wild type. We have shown that 6-hydroxycholest-4-en-3-one is a decomposition product of cholest-5-en-3-one (*30*). The presence of 2% 6-hydroxycholest-4-en-3-one in the wild-type reaction suggests to us that in one in every 50 catalytic reactions, the enzyme releases intermediate cholest-5-en-3-one. The Δ^{79-83} mutant has the same ratio. On the basis of these experiments, we conclude that deletion of the looplet residues does not affect the grip of the enzyme on the intermediate.

Next we examined the ability of the Δ^{79-83} enzyme to transfer the 4β proton during the isomerization reaction using [4β-^{2}H]cholesterol. In the wild-type-catalyzed reaction, 30% of the deuterium at the 4β-position is transferred to the 6β-position (*30*). The remaining 70% is washed-out, lost to solvent. The results of this experiment were consistent with the role of glutamate 361 as the single base responsible for isomerization of the intermediate cholest-5-en-3-one to cholest-4-en-3-one. When the experiment was conducted with the Δ^{79-83} mutant, the amount of deuterium transferred decreased. Twenty-two percent of the deuterium label at the 4β-carbon was transferred to the 6β-carbon. This experiment confirmed that the catalytic function of the base was not perturbed by the loop truncation. Furthermore, the access of the active site when steroid is bound to bulk solvent is only slightly increased by deletion of the five loop residues; i.e., we do not see complete wash-out of the deuterium label.

These two experiments suggest that the major role of the looplet is not sequestration or protection of the intermediate(s) from bulk solution. We next analyzed the catalytic activity of the mutant enzyme with a soluble, monomeric substrate, dehydroepiandrosterone (Chart 1). DHEA has the same A/B-ring functionality as cholesterol: a 3β-hydroxyl and a 5,6 double bond. It differs at C_{17}; DHEA has a ketone and cholesterol has an eight carbon "tail". As a consequence, DHEA is more soluble in aqueous solutions than cholesterol and is assayed in 10% EtOH. The Δ^{79-83} mutant has the same k_{cat} for DHEA as wild type (Table 1). Moreover, the K_m is improved, i.e., lower, compared to wild type. Hence, the mutant enzyme is 6-fold *more* specific for DHEA than wild type. Comparison of the mutant and wild type steady-

state rate constants indicates that the mutant enzyme is still catalytically active.

Due to the limited solubility of cholesterol, it is assayed as a mixed micelle with 2% propan-2-ol and 0.025% Triton X-100. The assay concentrations are at the critical micelle concentration of Triton X-100 (*35*) and above the critical micelle concentration of cholesterol (*36*). Deletion of the five loop residues reduces the k_{cat} for cholesterol 13-fold. In addition, the K_m is increased at least 14-fold. The K_m is difficult to measure accurately because the concentration is nearing the solubility limit of cholesterol. The net result is that the mutant enzyme is 180-fold *less* specific for cholesterol than wild type (Table 1). The lowered specificity for cholesterol may be interpreted in two ways. Either deletion of the loop residues has eliminated some of the cholesterol binding site or deletion has reduced the affinity of the enzyme for aggregated substrate surfaces. The increased specificity for DHEA hints that some of the loop residues bind the eight-carbon C_{17}-tail of cholesterol and that deletion results in removal of the cholesterol tail binding site. Four of the deleted residues, phenylalanine 80, leucine 81, tryptophan 82, and leucine 83, face the active site in the DHEA-bound X-ray structure. The fifth, serine 79, faces the aqueous environment. In a cholesterol-bound conformation, i.e., loop open, these residues must pack with the eight-carbon C_{17}-tail of cholesterol. Thus, their deletion results in a lowered specificity for cholesterol. In the wild-type enzyme, these four hydrophobic residues have nonideal interactions with the C_{17}-ketone of DHEA. Upon their deletion, these unfavorable interactions are alleviated and the specificity for DHEA improves.

To address the issue of enzyme affinity for aggregated substrate surfaces, we studied the catalytic function of the Δ^{79-83} mutant with phospholipid vesicles, another form of aggregated substrate. We used 100-nm phospholipid/cholesterol vesicles prepared by extrusion to ensure homogeneity. The rate of cholesterol oxidation catalyzed by cholesterol oxidase with vesicle substrates is much faster than the rate of sterol desorption from the lipid bilayer (*37*−*39*). The maximum initial rate of turnover, i.e., when 100% of the enzyme is bound to the vesicles, is 24 s^{-1} (Table 2). In comparison, the rate of cholesterol desorption from 100-nm vesicles in the absence of enzyme is approximately 2×10^{-5} s^{-1} (*40*, *41*). Consequently, from a kinetic argument, cholesterol oxidase must associate with the lipid bilayer before binding substrate. The enzyme does not wait for cholesterol to desorb from the membrane and bind cholesterol from aqueous solution; rather it facilitates the extraction of cholesterol from the membrane. The apparent dissociation constant for enzyme and vesicles is measured kinetically by monitoring the increase in initial velocity as a function of bulk vesicle (1:1, ePC/cholesterol) concentration. We also measured the dissociation constant of cholesterol oxidase for vesicles using an independent physical method, fluorescence. The quenching of intrinsic tryptophan fluorescence upon binding to phospholipid vesicles saturates and a fit of the curve yields K_D for phospholipid vesicles (Table 2).

Comparison of the wild type and Δ^{79-83} mutant dissociation constants reveals that deletion of the five loop residues slightly weakens the affinity of the enzyme for the membrane. Whether measured kinetically or fluorimetrically, the binding constant increases 2-fold. The dramatic difference

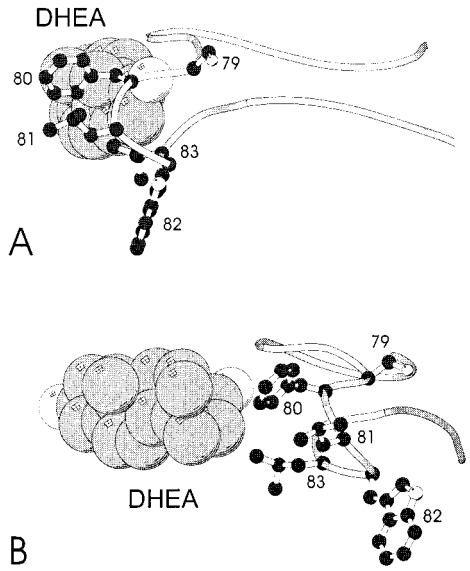

FIGURE 4: Models of *Streptomyces* loop 70−90 with DHEA bound in the active site and side chains that are deleted in Δ^{79-83} displayed. Amino acid side chains corresponding to the choA sequence were substituted for the *B. sterolicum* residues in the choB structure (1COY) without any minimization. These residues are believed to form a hydrophobic pathway between membrane and active site for binding cholesterol. (A) The same view of loop 70−90 as shown in Figure 1A. (B) Same as (A) except the structure has been rotated 45° about the *y*-axis.

arises in comparison of the catalytic activities at saturation of binding. The Δ^{79-83} mutant initial velocity is 0.0087 s^{-1} as compared to 24 s^{-1} with wild type. That is, when all of the Δ^{79-83} mutant enzyme is bound to the vesicle, the mutant binds cholesterol, oxidizes, and isomerizes it to cholest-4-en-3-one and releases it 3000 times more slowly than wild type. The ease with which Δ^{79-83} converts DHEA to androsterone implies that loop truncation does not interfere with the chemical steps. Rather, the loop is necessary for substrate binding and product release. The reduced specificity of the mutant enzyme for micellar cholesterol hints at this requirement. The minimal activity with vesicle substrates underlines the importance of the loop for extracting cholesterol out of the membrane.

Previously, we tested whether the interaction of the open conformation of the putative active site lid with the membrane was sufficiently disruptive of the membrane structure to cause leakage or lysis of the cell membrane. We found that binding of cholesterol oxidase to lipid vesicles does not cause leakage of encapsulated dye, implying that the membrane is not disrupted upon binding (*25*). This evidence taken in combination with the relatively weak binding of wild type to vesicles suggests that the enzyme rests on the surface of the lipid bilayer with the large loop open to form a hydrophobic pathway (Figure 4). With direct movement of cholesterol from the membrane to the enzyme binding site, solvation of sterol by water is obviated, and consequently, the transition states for cholesterol release from the membrane and cholest-4-en-3-one insertion are lowered. Deletion of the four amino acids, phenylalanine 80, leucine 81, tryptophan 82, and leucine 83, that line the pathway at the tip of the loop destroys part of the hydrophobic pathway, and the rate of catalytic turnover with membrane substrate drops markedly. The initial velocity is only 400-fold faster than the rate of noncatalyzed sterol desorption from the

membrane. Without the tip of the loop, the substrate and product must be exposed to solvent upon binding and release, respectively, and the corresponding transition state energies of these processes are increased.

Additional evidence for a hydrophobic pathway was reported by Loubat-Hugel and co-workers (*42*). In their work, they discovered that methionine oxidation of *B. sterolicum* cholesterol oxidase changes the specificity of the enzyme. The oxidized enzyme is no longer catalytically active with micellar cholesterol. However, it has the same k_{cat}/K_m as wild type for DHEA and 3β-hydroxy-17β-androst-5-ene carboxylic acid, soluble, monomeric substrates. However, they do not know which of 14 methionines in the protein are oxidized. In light of our results, it seems likely that oxidation of methionine 81 (leucine 81 in the *Streptomyces* sequence) is responsible for the change in specificity. Transformation of the methionine in the loop to a sulfoxide would decrease the hydrophobicity of the hydrophobic pathway and alter the loop so that it no longer packs optimally with cholesterol.

Thus, it appears that cholesterol oxidase utilizes an active site lid in a manner similar to the lipases. Both enzymes are water soluble and have amphipathic lids that protect their hydrophobic active sites and confer specificity. The lids open at the lipid interface to present their active sites to their respective lipid substrates. The role of the lipase lid, however, appears to be 2-fold. In addition to conferring specificity, it is required for binding to the interface (*15*, *43*, *44*). The amphipathic lids of cholesterol oxidase and lipase represent one structural motif for enzymes that hydrolyze highly hydrophobic substrates yet are soluble in the aqueous milieu. Phospholipase A_2 and cholesterol esterase utilize two different motifs. The binding site of cholesterol esterase is a deep hydrophobic gorge that is formed by dimerization of the protein. The X-ray crystal structures suggest that in the absence of substrate the hydrophobic surface is protected from solvent by slight rotation of the monomers with respect to one another, i.e., a quarternary structure change (*45*). The active site of phospholipase A_2 is not protected by a lid or protein interface. Instead, small adjustments in the position of aromatic side chains in the active site occur upon substrate binding (*46*). In addition, binding to the interface stabilizes the conformation of the N-terminal residues and the active site residues (*47*). Hence, the most polar phospholipids require minor structural changes compared to the very hydrophobic cholesteryl fatty acid esters. Triacylglycerides and cholesterol are of intermediate hydrophobicity, requiring moderate conformational changes, i.e., active site lids. These examples suggest that the hydrophobicity of the substrate dictates the molecular architecture required for its binding (*48*).

More detailed discussion about cholesterol oxidase must await crystallographic information about the liganded mutant enzyme and the open wild-type enzyme. The exact structure of the open loop is still not known, nor is it known if loop 70−90 possesses hinge residues or opens in a shear motion (*49*). It is clear that the looplet 79−83 is necessary for packing with the "tail" of cholesterol as previously deduced from the crystal structure (*18*). The catalytic chemistry of the enzyme is left intact upon deletion of the five loop-tip residues. With lipid vesicle substrates, the loop is important for extraction of cholesterol from the membrane and is not the primary determinant of binding affinity for vesicles.

ACKNOWLEDGMENT

We thank Weiqun Zhu for initial work on this project, Xiaoyu Chen for assisting with the fluorescence measurements, and Prof. Y. Murooka for kindly providing the pCO117 clone of cholesterol oxidase. We also thank Professor Suzanne Scarlata for helpful discussion and the use of her spectrofluorometer.

REFERENCES

1. Kempner, E. S. (1993) *FEBS Lett. 326*, 4−10.
2. Fetrow, J. S. (1995) *FASEB J. 9*, 708−717.
3. Leszczynski, J. F., and Rose, G. D. (1986) *Science 234*, 849−855.
4. Koshland, D. E., Jr. (1958) *Proc. Natl. Acad. Sci. U.S.A. 44*, 98−104.
5. Herschlag, D. (1988) *Bioorg. Chem. 16*, 62−96.
6. Clarke, A. R., Wigley, D. B., Chia, W. N., Barstow, D., Atkinson, T., and Holbrook, J. J. (1986) *Nature (London) 324*, 699−702.
7. First, E. A., and Fersht, A. R. (1993) *Biochemistry 32*, 13658−13663.
8. Li, L., Falzone, C. J., Wright, P. E., and Benkovic, S. J. (1992) *Biochemistry 31*, 7826−7833.
9. Kato, H., Tanaka, T., Yamaguchi, H., Hara, T., Nishioka, T., Katsube, Y., and Oda, J. (1994) *Biochemistry 33*, 4995−4999.
10. Pompliano, D. L., Peyman, A., and Knowles, J. R. (1990) *Biochemistry 29*, 3186−3194.
11. Larson, E. M., Larimer, F. W., and Hartman, F. C. (1995) *Biochemistry 34*, 4531−4537.
12. Fetrow, J. S., Horner, S. R., Oehrl, W., Schaak, D. L., Boose, T. L., and Burton, R. E. (1997) *Protein Sci. 6*, 197−210.
13. Pullybank-Mulligan, P., Spitzer, J. S., Gilden, B. M., and Fetrow, J. S. (1996) *J. Biol. Chem. 271*, 8633−8645.
14. Yang, X.-J., and Miles, W. W. (1992) *J. Biol. Chem. 267*, 7520−7528.
15. Carrière, F., Thirstrup, K., Hjorth, S., Ferrato, F., Nielsen, P. F., Withers-Martinez, C., Cambillau, C., Boel, E., Thim, L., and Verger, R. (1997) *Biochemistry 36*, 239−248.
16. Egloff, M.-P., Marguet, F., Buono, G., Verger, R., Cambillau, C., and Tilbeurgh, H. V. (1995) *Biochemistry 34*, 2751−2762.
17. Derewenda, U., Brzozowski, A. M., Lawson, D. M., and Derewenda, Z. S. (1992) *Biochemistry 31*, 1532−1541.
18. Li, J., Vrielink, A., Brick, P., and Blow, D. M. (1993) *Biochemistry 32*, 11507−11515.
19. Vrielink, A., Lloyd, L. F., and Blow, D. M. (1991) *J. Mol. Biol. 219*, 533−554.
20. Ishizaki, T., Hirayama, N., Shinkawa, H., Nimi, O., and Murooka, Y. (1989) *J. Bacteriol. 171*, 596−601.
21. Ohta, T., Fujishiro, K., Yamaguchi, K., Tamura, Y., Aisaka, K., Uwajima, T., and Hasegawa, M. (1991) *Gene 103*, 93−96.
22. Nomura, N., Choi, K.-P., and Murooka, Y. (1995) *J. Ferm. Bioeng. 79*, 410−416.
23. Sambrook, J., Fritsch, E. F., and Maniatis, T. (1989) *Molecular cloning*: *a laboratory manual*, 2nd ed., Cold Spring Harbor Laboratory Press, Cold Spring Harbor, New York.
24. Sanger, F., Niklen, S., and Coulson, A. R. (1977) *Proc. Natl. Acad. Sci. U.S.A. 74*, 5463−5467.
25. Ghoshroy, K. B., Zhu, W., and Sampson, N. S. (1997) *Biochemistry 36*, 6133−6140.
26. Fasman, G. D. (1992) *Practical Handbook of Biochemistry and Molecular Biology*, C. R. C. Press, Boca Raton, FL.
27. Hope, M. J., Bally, M. B., Webb, G., and Cullis, P. R. (1985) *Biochim. Biophys. Acta 812*, 55−65.
28. Stewart, J. C. M. (1959) *Anal. Biochem. 104*, 10−14.
29. Smith, A. G., and Brooks, C. J. W. (1977) *Biochem. J. 167*, 121−129.
30. Sampson, N. S., and Kass, I. J. (1997) *J. Am. Chem. Soc. 119*, 855−862.

31. Kass, I. J., and Sampson, N. S. (1995) *Biochem. Biophys. Res. Commun. 206*, 688−693.
32. Purcell, J. P., Greenplate, J. T., Jennings, M. G., Ryerse, J. S., Pershing, J. C., Sims, S. R., Prinsen, M. J., Corbin, D. R., Tran, M., Sammons, R. D., and Stonard, R. J. (1993) *Biochem. Biophys. Res. Commun. 196*, 1406−1413.
33. Greenplate, J. T., Duck, N. B., Pershing, J. C., and Purcell, J. P. (1995) *Entomol. Exp. Appl. 74*, 253−258.
34. Lange, Y. (1992) *J. Lipid Res. 33*, 315−321.
35. Schick, M. J., Atlas, S. M., and Eirich, F. R. (1962) *J. Phys. Chem. 66*, 1326−1333.
36. Haberland, M. E., and Reynolds, J. A. (1973) *Proc. Natl. Acad. Sci U.S.A. 70*, 2313−2316.
37. Phillips, M. C., Johnson, W. J., and Rothblat, G. H. (1987) *Biochim. Biophys. Acta 906*, 223−276.
38. Lund-Katz, S., Laboda, H. M., McLean, L. R., and Phillips, M. C. (1988) *Biochemistry 27*, 3416−3423.
39. Bar, L. K., Chong, P. L.-G., Barenholz, Y., and Thompson, T. E. (1989) *Biochim. Biophys. Acta 983*, 109−112.
40. Rodrigueza, W. V., Wheeler, J. J., Klimuk, S. K., Kitson, C. N., and Hope, M. J. (1995) *Biochemistry 34*, 6208−6217.
41. McLean, L. R., and Phillips, M. C. (1981) *Biochemistry 20*, 2893−2900.
42. Loubat-Hugel, C., Tritsch, D., and Biellmann, J. F. (1994) *C. R. Acad. Sci., Ser. III 317*, 299−303.
43. Thirstrup, K., Verger, R., and Carrière, F. (1994) *Biochemistry 33*, 2748−2756.
44. Bengtsson, G., and Olivecrona, T. (1981) *Eur. J. Biochem. 113*, 547−554.
45. Ghosh, D., Wawrzak, Z., Pletnev, V. Z., Li, N., Kaiser, R., Pangborn, W., Jornvall, H., Erman, M., and Duax, W. L. (1995) *Structure 3*, 279−288.
46. Scott, D. L., White, S. P., Otwinowski, Z., Yuan, W., Gelb, M. H., and Sigler, P. B. (1990) *Science 250*, 1541−1546.
47. van den Berg, B., Tessari, M., Boelens, R., Dijkman, R., de Haas, G. H., Kaptein, R., and Verheij, H. M. (1995) *Struct. Biol. 2*, 402−406.
48. Cambillau, C., Longhi, S., Nicolas, A., and Martinez, C. (1996) *Curr. Opin. Struct. Biol. 6*, 449−455.
49. Gerstein, M., Lesk, A. M., and Chothia, C. (1994) *Biochemistry 33*, 6739−6749.
50. Kraulis, P. J. (1991) *J. Appl. Crystal. 24*, 946−950.

BI973067G